

by using a Corning combination pH electrode with a Orion Model 701 pH meter standardized with buffers at pH 7.0 and 10.00.

General Procedure for Homogeneous Esterolysis Reactions. Three milliliters of the aqueous buffer at the desired pH was pipetted into a cuvette. The substrates were dissolved in acetonitrile to make solutions at concentrations such that injection of 1 μ L of the solution into the buffer in the cuvette would result in a substrate concentration of 1×10^{-5} M. The polymer and PPY were dissolved in methanol to obtain solutions such that each microliter when injected into 3 mL of buffer yielded a catalyst concentration of 5×10^{-7} M. For catalyzed reactions the desired amount of catalyst was injected into the cuvette and the contents were shaken to ensure mixing. The cuvette was introduced into the UV

(31) Weast, R. C., Ed. *Handbook of Chemistry and Physics*, 64th ed. CRC: Boca Raton, FL, 1984, p D-150.

spectrometer and the stirrer started. The data acquisition programs were loaded into the computer along with a data disk in the appropriate drive. The desired amount of substrate was injected and a stopwatch started. After exactly 1 min, data acquisition was initiated. Spectra were collected at time intervals of 3, 5, or 60 min depending on the experiment. After the required number of spectra had been collected, the data analysis routine was initiated and the absorbance at 400 nm was determined as a function of time. Knowing the extinction coefficient for the *p*-nitrophenoxide ion and the initial substrate concentration, we calculated the conversion of substrate. Each kinetic run was repeated at least 3 times.

Acknowledgment. Grateful acknowledgment is made to 3M and to the donors of the Petroleum Research Fund, administered by the American Chemical Society, for financial support of this research.

Esterolytic Chemistry of a Vesicular Thiocholine Surfactant

Robert A. Moss,* Thomas F. Hendrickson, and George O. Bizzigotti

Contribution from the Wright and Rieman Laboratories, Department of Chemistry, Rutgers, The State University of New Jersey, New Brunswick, New Jersey 08903. Received February 27, 1986

Abstract: The thiol-functionalized surfactant *N,N*-dihexadecyl-*N*-methyl-*N*-(2-mercaptoethyl)ammonium chloride (**2**) (16_2SH ; $16 = n\text{-C}_{16}\text{H}_{33}$) was synthesized. Vesicles prepared from 16_2SH were characterized by electron microscopy, gel filtration, dynamic light scattering, differential scanning calorimetry, and permeability toward 1-anilino-8-naphthalenesulfonate (fluorescence stopped-flow spectroscopy). Excess vesicular 16_2SH in aqueous solution at pH 7.7 cleaved various activated ester substrates; k_v^{max} values (s^{-1}) are as follows: *p*-nitrophenyl acetate, 4.9; *p*-nitrophenyl hexanoate, 13.4; 4-acetoxy-3-nitrobenzenesulfonate, 7.3; and *p*-nitrophenyl palmitate, 21.7. Second-order rate constants ranged up to ~ 9000 L/(mol·s) for the hexanoate and ~ 9800 L/(mol·s) for the sulfonate substrates. At short reaction times, with hydrophobic substrates, deprotonation (to 16_2S^-) and attendant structural changes of the 16_2SH vesicles are rate limiting under reaction conditions where the pH is "jumped" from 2.0 to 7.7. After ~ 200 ms at pH 7.7, 16_2S^- thiolate cleavage of the substrates becomes rate limiting. Artifacts processes that mimic the reaction are identified at "long" reaction times (~ 10 – 100 s).

The introduction of functional surfactants was crucial to the development of micellar reagents as reaction catalysts and enzyme models.¹ A similar period in vesicular chemistry began about 1980 and has steadily gained momentum.² Exclusive of surfactants with unsaturated hydrocarbon moieties, intended for the preparation of polymerized vesicles,³ many other functional vesicle-forming surfactants have been synthesized.^{2,4} Frequently, these have been derived from amino acids,⁵ but "unnatural" functionalities have also been incorporated. These include aryldiazonium,⁶ azo,⁷ carbazole,⁸ isonitrile,⁹ pyridinioamidate,¹⁰

pyridoxal,¹¹ and viologen.¹²

Due to their importance in the chemistry of hydrolytic enzymes and the desire to develop vesicular chemistry along biomimetic lines,² special attention has been devoted to the imidazole and thiol functional groups. This has led to esterolytic reagents that feature imidazole derivatives noncovalently bound to dialkyldimethylammonium ion vesicles,¹³ hydrophobic histidine derivatives that mediate stereoselective vesicular esterolyses,¹⁴ and functional vesicle-forming surfactants synthesized from histidine.^{5b,15} Recently, we introduced the simple imidazole ester surfactant **1** (16_2Im) and characterized its kinetic properties in the vesicular cleavage of several substrates.¹⁶

(1) (a) Fendler, J. H.; Fendler, E. J. *Catalysis in Micellar and Macromolecular Systems*; Academic: New York, 1975. (b) Tonellato, U. *In Solution Chemistry of Surfactants*; Mittal, K. L., Ed.; Plenum: New York, 1979; Vol. II, p 541 ff. (c) Kunitake, T.; Shinkai, S. *Adv. Phys. Org. Chem.* **1980**, *17*, 435. (d) O'Connor, C. J.; Ramage, R. E.; Porter, A. J. *Adv. Colloid Interface Sci.* **1981**, *15*, 25.

(2) Fendler, J. H. *Membrane Mimetic Chemistry*; Wiley: New York, 1982. Fendler, J. H. *Acc. Chem. Res.* **1980**, *13*, 7.

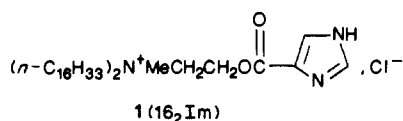
(3) Review: Fendler, J. H.; Tundo, P. *Acc. Chem. Res.* **1984**, *17*, 3. For leading references, see also: Elbert, R.; Laschewsky, A.; Ringsdorf, H. *J. Am. Chem. Soc.* **1985**, *107*, 3134. Regen, S. J.; Shin, J.-S.; Yamaguchi, K. *Ibid.* **1984**, *106*, 2446. Nome, F.; Reed, W.; Politi, M.; Tundo, P.; Fendler, J. H. *Ibid.* **1984**, *106*, 8086. Kunitake, T.; Nakashima, N.; Takarabe, K.; Nagai, M.; Tsuge, A.; Yanagi, H. *Ibid.* **1981**, *103*, 5945.

(4) Review: Fuhrhop, J.-H.; Mathieu, J. *Angew. Chem., Int. Ed. Engl.* **1984**, *23*, 100.

(5) (a) Murakami, Y.; Nakano, A.; Yoshimatsu, A.; Uchitomi, K.; Matsuda, Y. *J. Am. Chem. Soc.* **1984**, *106*, 3613. (b) Kunitake, K.; Ihara, H.; Okahata, Y. *Ibid.* **1983**, *105*, 6070. (c) Murakami, Y.; Nakano, A.; Ikeda, H. *J. Org. Chem.* **1982**, *47*, 2137. (d) Murakami, Y.; Aoyama, Y.; Kikuchi, J.-i.; Nishida, K.; Nakano, A. *J. Am. Chem. Soc.* **1982**, *104*, 2937.

(6) Fuhrhop, J.-H.; Bartsch, H. *Liebigs Ann. Chem.* **1983**, 802. Fuhrhop, J.-H.; Bartsch, H.; Fritsch, D. *Angew. Chem., Int. Ed. Engl.* **1981**, *20*, 804. Moss, R. A.; Shin, J.-S. *J. Chem. Soc., Chem. Commun.* **1983**, 1027.

(7) Shimomura, M.; Kunitake, T. *J. Am. Chem. Soc.* **1982**, *104*, 1757.



(8) Kunitake, T.; Shimomura, M.; Hashiguchi, Y.; Kawanaka, T. *J. Chem. Soc., Chem. Commun.* **1985**, 833.

(9) Roks, M. F. M.; Visser, H. G. J.; Zwikker, J. W.; Verkleij, A. J.; Nolte, R. J. M. *J. Am. Chem. Soc.* **1983**, *105*, 4507.

(10) Haubs, M.; Ringsdorf, H. *Angew. Chem., Int. Ed. Engl.* **1985**, *24*, 882.

(11) Murakami, Y.; Kikuchi, J.-i.; Imori, T.; Akiyoshi, K. *J. Chem. Soc., Chem. Commun.* **1984**, 1434.

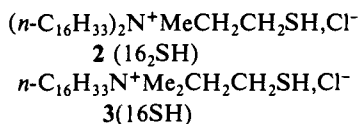
(12) Baumgartner, E.; Fuhrhop, J.-H. *Angew. Chem., Int. Ed. Engl.* **1980**, *19*, 550. Tundo, P.; Kurihara, K.; Kippenberger, J.; Politi, M.; Fendler, J. H. *Ibid.* **1982**, *21*, 81.

(13) Kunitake, T.; Sakamoto, T. *J. Am. Chem. Soc.* **1978**, *100*, 4615. Kunitake, T.; Sakamoto, T. *Chem. Lett.* **1979**, 1059.

(14) Ueoka, R.; Matsumoto, Y.; Ninomlya, Y.; Nakagawa, Y.; Inoue, K.; Ohkubo, K. *Chem. Lett.* **1981**, 785. Ohkubo, K.; Matsumoto, N.; Ohta, H. *J. Chem. Soc., Chem. Commun.* **1982**, 739.

(15) Murakami, Y.; Nakano, A.; Yoshimatsu, A.; Fukuya, S. *J. Am. Chem. Soc.* **1981**, *103*, 728.

Related chemistry of the thiol moiety was first explored by Chaimovich et al., who reported a kinetic study of the cleavage of *p*-nitrophenyl esters by heptanethiol noncovalently bound to dialkyldimethylammonium ion vesicles.¹⁷ In 1981, we communicated the synthesis of the functional thiol surfactant **2** (16₂SH),



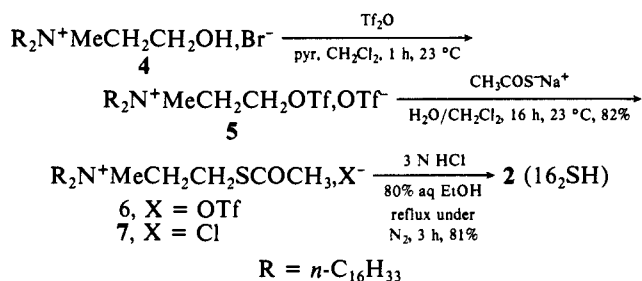
as well as some physical and esterolytic properties of the vesicles derived from it.¹⁸ Subsequently, Bizzigotti described the reactions of 16₂SH with Ellman's reagent.¹⁹ Recently, Regen has prepared bis thiol functional surfactants related to both phosphatidylcholines and to 16₂SH.²⁰

Now we present a full report on the vesicular esterolytic properties of 16₂SH toward a variety of substrates. In particular, we highlight the unusual behavior observed at very short reaction times, where zero-order reactions are observed with hydrophobic substrates. These reactions derive from rate-limiting vesicular changes that accompany an imposed pH jump and a consequent ionization of the vesicles' SH head groups.

Results

Synthesis. The preparation of 16₂SH is outlined in Scheme I¹⁸ and closely follows that of its single-chain, micelle-forming analogue **3** (16SH).^{21,22} The dihexadecylcholine surfactant **4**²³ was converted to its triflate **5** which, without isolation, was stirred in CH₂Cl₂ solution with aqueous sodium thioacetate at pH 7.5. The ensuing "self phase transfer" catalytic reaction afforded the substitution product **6**.²⁴ Surfactant triflate salt **6** was ion exchanged to the water-soluble chloride salt **7** with Dowex 1-X8 beads in 80% aqueous ethanol at 75 °C. Finally, **7** was deprotected with O₂-free, aqueous ethanolic HCl, affording 16₂SH that was isolated by lyophilization and purified by recrystallization from EtOAc.

Scheme I



Surfactant 16₂SH displayed quantitative SH reactivity toward Ellman's reagent,²⁵ but it was very sensitive toward oxidation. Accordingly, it was stored under high vacuum, and its solutions were always freshly prepared in N₂-purged distilled water, adjusted to pH 2 with HCl. (The anionic 16₂S⁻ form is much more sensitive to oxidation than the fully protonated 16₂SH.) Preparative details and spectroscopic characterizations of surfactants **2** and **5–7** appear in the Experimental Section.

Vesicle Formation and Characterization. Vesicles of 16₂SH were prepared by injecting^{17a,26} ethanolic solutions of the surfactant into warm, acidic, N₂-purged distilled water. For example, 0.15 mL of a 0.016 M ethanolic solution of 16₂SH was injected through a heat-drawn microcapillary tube (exit aperture <0.1 mm) into 3.0 mL of 0.009 M aqueous HCl containing 0.017 M KCl. The aqueous solution was maintained at 55–60 °C during the injection. Subsequent cooling to 25 °C afforded optically clear solutions of vesicular 16₂SH. Later, we found that equivalent injected vesicles could be prepared using a Yale No. 25 stainless steel syringe needle. Sonication was not useful in vesicle preparation because it induced extensive oxidative dimerization of the surfactant.

Several physical methods were used to characterize the vesicles. Electron microscopy of vesicles prepared by injection of 16₂SH into 2% aqueous uranyl acetate solution (pH ~4) revealed multilamellar vesicles with diameters of 1000–3000 Å and bilayer widths of 30–40 Å.²⁷ Gel filtration of 16₂SH vesicles, carrying entrapped 6-carboxyfluorescein, on Sephadex G-25-80 gave elution results consistent with those for vesicles of at least 1000 Å in diameter¹⁸ (*d*). Dynamic light scattering measurements²⁸ of 1–2 mM 16₂SH vesicle solutions gave a range of mean hydrodynamic diameters depending on the solution's pH and history. Solutions prepared by injection of ethanolic 16₂SH into Tris buffer at pH 7.5 gave vesicles with *d* ~ 1430 Å. For vesicles prepared at pH 2, and subsequently adjusted to pH 7.5 with Tris, *d* was ~970 Å. These values are in reasonable agreement with the gel filtration and electron microscopic results, and a similar *d* (1100 Å) has been measured for injected vesicles of the nonfunctional quaternary ammonium ion surfactant (n-C₁₆H₃₃)₂N⁺Me₂,Br⁻ (16₂).²⁹

At pH 2, however, vesicular 16₂SH gave much smaller diameters by light scattering, typically ~320 Å. From the rate constant vs. pH dependence of the vesicular 16₂SH cleavage of *p*-nitrophenyl acetate in 0.01 M KCl solution, we find pK_a ~7.3, equivalent to that of micellar 16SH,²¹ so that the charge type of vesicular 16₂SH changes from cationic at pH 2 to predominantly zwitterionic at pH 7.5. This may affect the mean translational diffusion coefficient of the vesicles and, hence, the apparent mean hydrodynamic diameter. We note that vesicle diameters from the electron micrographs of 16₂SH vesicles prepared at pH 4 are much larger than those of the pH 2 vesicles observed in solution by light scattering. It is not known, however, whether vesicle drying preparatory to electron microscopy affects the vesicle diameter.

Differential scanning calorimetry of 0.015 M vesicular 16₂SH in 0.02 M, pH 7.5 aqueous Tris buffer revealed a reversible gel to liquid crystalline phase transition with Δ*H* = 2.4 kcal/mol, *T*_c = 35.25 °C, a van't Hoff enthalpy of 450 kcal/mol, and a cooperativity of 190 molecules of 16₂SH.^{18,30}

We also characterized the permeabilities of vesicular 16₂SH and 16₂OH (**4**) toward the transmembrane transport of 1-anilino-8-naphthalenesulfonate (ANS). These experiments were done by stopped-flow fluorescence spectroscopy and take the time-dependent development of ANS fluorescence upon stopped-flow mixing of aqueous ANS and vesicular solutions as a kinetic measure of the transport or permeation of the ANS across the exovesicular surface and outer bilayer.^{29,31}

Static fluorescence emission maxima were first determined for 5 × 10⁻⁵–1 × 10⁻⁴ M ANS, solubilized in various 1 × 10⁻³ M vesicular surfactant solutions. We observed a λ_{max}^{em} of 476 nm in 16₂ at pH 7.4, 469 nm in 16₂OH at pH 2 (468 nm at pH 7.7),

(26) Batzli, S.; Korn, E. D. *Biochim. Biophys. Acta* **1973**, *298*, 1015.

(27) The electron micrograph appears in ref 18. We thank L. Flores for this determination.

(28) Light-scattering data were collected at 25 °C and a 90° scattering angle with a Nicomp Model TC-100 computing autocorrelator, an argon laser light source (488 nm), and a Hazeltine microcomputer that used the cumulant program.

(29) Moss, R. A.; Hendrickson, T. F.; Swarup, S.; Hui, Y.; Marky, L.; Breslauer, K. J. *Tetrahedron Lett.* **1984**, *25*, 4063.

(30) We thank Dr. L. Marky and Prof. E. Breslauer for this determination.

(31) Haynes, D. H.; Simkowitz, P. J. *Membr. Biol.* **1977**, *33*, 63 and references therein.

(16) Moss, R. A.; Kim, K. Y. *Isr. J. Chem.* **1985**, *25*, 11.

(17) (a) Cuccovia, I. M.; Aleixo, R. M. V.; Mortara, R. A.; Filho, P. B.; Bonilha, J. B. S.; Quina, F. H.; Chaimovich, H. *Tetrahedron Lett.* **1979**, 3065.

(b) Cuccovia, I. M.; Quina, F. H.; Chaimovich, H. *Tetrahedron* **1982**, *38*, 917.

(18) Moss, R. A.; Bizzigotti, G. O. *J. Am. Chem. Soc.* **1981**, *103*, 6512.

(19) Bizzigotti, G. O. *J. Org. Chem.* **1983**, *48*, 2598.

(20) Regen, S. L.; Yamaguchi, K.; Samuel, N. K. P.; Singh, M. J. *Am. Chem. Soc.* **1983**, *105*, 6354.

(21) Regen, S. L. *Ibid.* **1985**, *107*, 42.

(22) Regen, S. L.; Samuel, N. K. P.; Khurana, J. M. *Ibid.* **1985**, *107*, 5804.

(23) Moss, R. A.; Bizzigotti, G. O.; Huang, C.-W. *J. Am. Chem. Soc.* **1979**, *102*, 754.

(24) See also: Moss, R. A.; Bizzigotti, G. O.; Lukas, T. J.; Sanders, W. J. *Tetrahedron Lett.* **1978**, 3661.

(25) Anoardi, L.; Fornasier, R.; Sostero, D.; Tonellato, U. *Gazz. Chim. Ital.* **1978**, *108*, 707.

(26) For preparative details, see: Moss, R. A.; Ihara, Y. *J. Org. Chem.* **1983**, *48*, 588 and ref 22 and 23 contained therein.

(27) Moss, R. A.; Sanders, W. J. *J. Am. Chem. Soc.* **1978**, *100*, 5247.

(28) Habeeb, A. F. S. A. *Methods Enzymol.* **1972**, *25*, 457.

Table I. Development of ANS Fluorescence in Vesicles^a

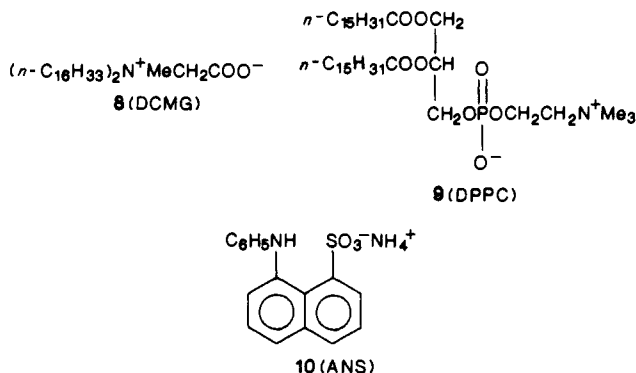
vesicle	pH	$\tau_{1/2}$ for fluorescence development, s
16 ₂ ^b	7.4	0.19
16 ₂ OH	2.0	0.091 ± 0.006 ₃ ^c
16 ₂ OH	7.7 ^d	0.192 ± 0.008 ₂
16 ₂ SH	2.0	0.014 ± 0.004 ₇
16 ₂ SH	7.7 ^d	0.011 ± 0.004 ₆ , 42 ^e
DCMG (8) ^f	7.4	0.31
DPPC (9)	7.4	g

^aDurrum D-130 stopped-flow spectrometer modified for fluorescence (90°), 150-W Xe excitation lamp, 25 °C. Final concentrations: [vesicles] = 5 × 10⁻⁴ M, [ANS] = 5 × 10⁻⁵ M. ^bData for injected (1100 Å) 16₂ vesicles at 23 °C, ref 29. ^cErrors are average deviations of *n* (subscript) measurements. ^dThe pH "jumped" upon mixing the vesicles in pH 2.0 HCl with 0.01 M Tris buffer (containing the ANS). ^eThis entry refers to a slow, subsequent fluorescence that disappeared when the vesicle solution contained dithiothreitol; see text. ^fData from ref 32. ^gThere is no ANS permeation observed below *T_c* (~40 °C). At *T_c*, $\tau_{1/2}$ = 4.5. s; see ref 29.

and 461 nm in 16₂SH at pH 2 (459 nm at pH 7.7). On the basis of these results, a 420-nm cutoff filter was used in the kinetic studies of ANS fluorescence; all fluorescence above 420 nm was sensed by the phototube detector. Excitation was at 368 nm.

In the stopped-flow fluorescence experiments, aqueous solutions of "empty" vesicles were rapidly mixed (<1 ms) with ANS solutions. The results appear in Table I, together with selected data from other investigations.^{29,32} The development of ANS fluorescence intensity with time is not strictly first order, but the half times are usually taken as inversely related to the rate of transmembrane transport of the probe.³¹

The principal conclusion from Table I is that permeation of the large anionic probe ANS (10) is very rapid across the exovesicular lamella of the dialkylammonium ion vesicles of 16₂, 16₂OH, and 16₂SH. The presence of the hydroxyl functional

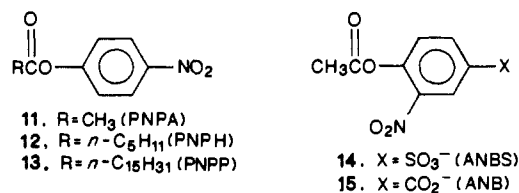


groups in 16₂OH has little effect on $\tau_{1/2}$, relative to the non-functional 16₂ vesicles. ANS permeation across 16₂SH vesicles is even faster than across 16₂ or 16₂OH at both pH 2 and 7.7. The latter observation is important because at pH 2 16₂SH vesicles will be cationic, whereas they will be largely zwitterionic at pH 7.7. Therefore the change in charge type does not greatly affect the rate of ANS transport. A similar conclusion was reached in our study of the dicetylmethylglycinate (DCMG) vesicles **8**.³² These zwitterionic vesicles afford a $\tau_{1/2}$ for ANS permeation similar to that of cationic 16₂.

Indeed, all of the R₂N⁺-based vesicles in Table I are characterized by relatively low $\tau_{1/2}$ values, in contrast to the zwitterionic, glycerol ester, dipalmitoylphosphatidylcholine vesicles (**9**, DPPC), where no ANS permeation occurs below the phase-transition temperature (~40 °C), and $\tau_{1/2}$ is on the order of seconds when it is observed.^{29,31} Thus, the permeation rates of ANS with the vesicular surfactants of Table I are mainly determined by backbone structure³² and are less affected by head group functionality or charge.

A peculiarity of the 16₂SH/ANS experiments is the appearance of a secondary fluorescence 10–20 s after the initial rapid fluorescence when the stopped-flow mixing involves the pH 2 to 7.7 jump. The secondary fluorescence has a $\tau_{1/2}$ of ~40–60 s and can be eliminated by the inclusion of 2 mM dithiothreitol in the 16₂SH vesicle preparation. We associate the secondary fluorescence with "disulfide" vesicles containing 16₂S–S16₂ surfactants. The thiol–disulfide oxidation is very rapid in basic vesicular solution;²⁰ its influence is also seen in kinetic studies of the 16₂SH/ester reactions (see below). Most likely, traces of dissolved oxygen, introduced during stopped-flow mixing, are responsible for this phenomenon. Inclusion of excess dithiothreitol, which reduces S–S to S⁻,²⁰ counteracts the oxidation and eliminates the secondary fluorescence.

Kinetics of Esterolysis. The esterolytic properties of vesicular 16₂SH were studied with several activated ester substrates that differed in hydrophobicity and charge type. These included *p*-nitrophenol acetate (**11**, PNPA), *p*-nitrophenyl hexanoate (**12**, PNPH), and *p*-nitrophenyl palmitate (**13**, PNPP), as well as the anionic substrates 4-acetoxy-3-nitrobenzenesulfonate (**14**, ANBS) and its benzoate analogue, **15** (ANB).



As we reported earlier, the pH 7.5 16₂SH vesicular cleavage of PNPA was kinetically biphasic, with two sequential, apparently first-order reactions, a "fast" process accounting for ≥90% of the absorbance change attributed to released *p*-nitrophenoxide ion (PNPO⁻) and a slower process accounting for the remaining Δ*A*¹⁸ (absorbance change). Similar experiments with substrates PNPH or PNPP revealed triphasic kinetic behavior: a rapid linear absorption increase lasting ~100 ms (zero-order phase), followed by a fast exponential absorbance increase of 0.1–2-s duration, and finally, a slow, apparently exponential signal that lasted for 1–2 min. These kinetic phases accounted for approximately 40%, 50%, and 10%, respectively, of the total time-dependent absorption.

We will consider separately each kinetic stage of the esterolysis reactions. For reasons outlined below, we identify the second, or fast, exponential phase as the "normal" nucleophilic thiolate esterolysis reaction. We believe that the initial zero-order phenomenon, observed only with the more hydrophobic PNPH and PNPP substrates, corresponds to rate-limiting changes in vesicular structure that accompany the pH jump imposed during the stopped-flow combination of vesicular 16₂SH at pH 2 and substrate/buffer solution at pH 8. With appropriate control experiments, we will demonstrate that the final, slow, first-order absorbance change is an artifact that is probably due to osmometric changes in the vesicles initiated by reagent combination.³³

Normal Exponential Stage. Vesicular 16₂SH was prepared by ethanolic injection (see above) into a 0.01 M aqueous KCl solution, adjusted to pH 2 with HCl. The vesicular solution was then reacted at 25 °C in a two-syringe, stopped-flow spectrophotometer (mixing time <1 ms) with a solution of 5 × 10⁻⁵ M substrate in 0.02 M aqueous Tris buffer, 0.01 M in KCl. After the mixing step, the final pH was 7.6–7.7, and final concentrations were [substrate] = 2.5 × 10⁻⁵ M, [Tris] = 0.01 M, [KCl] = 0.01 M, and ethanol ~ 4 vol %. Kinetics were followed by the absorbance of PNPO⁻ (or the aryl oxides from **14** or **15**) at 400 nm. Pseudo-first-order rate constants, *k_v* (>90% of reaction, *r* > 0.99), were generated by computer acquisition and analysis of absorption vs. time data.

Mean values of rate constants as a function of [16₂SH] appear in Table II for the fast exponential stages of the reactions (see above). Visual presentations of the *k_v*/[surfactant] profiles appear

(32) Moss, R. A.; Swarup, S.; Wilk, B.; Hendrickson, T. F. *Tetrahedron Lett.* **1985**, 26, 4827.

(33) Cf.: Moss, R. A.; Swarup, S.; Hendrickson, T. F.; Hui, Y. *Tetrahedron Lett.* **1984**, 25, 4079.

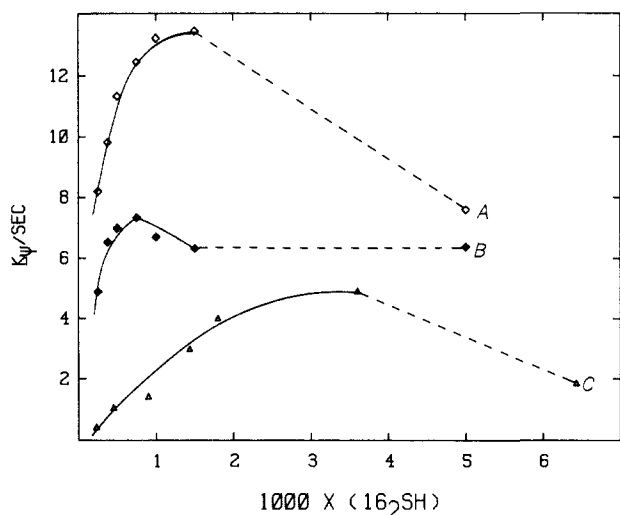


Figure 1. Pseudo-first-order rate constants k_p (s^{-1}) vs. $[16_2SH]$ (M) for the reactions at pH 7.6–7.7 of vesicular 16_2SH with PNPA (Δ), ANBS (\blacklozenge), and PNPB (\diamond); see text for conditions and Table II for data. Points A, B, and C serve to demonstrate that the maxima have been passed but are not included in Lineweaver–Burk calculations.

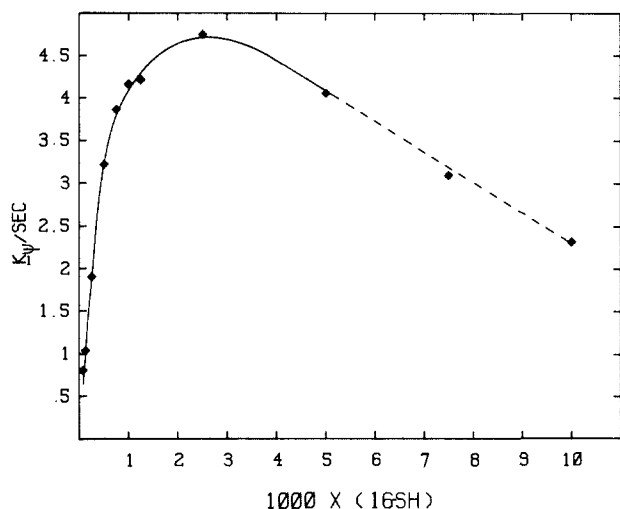


Figure 2. Pseudo-first-order rate constants k_p (s^{-1}) vs. $[16SH]$ (M) for the reaction of micellar $16SH$ with PNPB at pH 7.7; see text for other conditions.

in Figure 1 for the PNPA, PNPB, and ANBS reactions. Additionally, a single determination for substrate ANB (**15**) gave

Table II. Rate Constants for Reactions of Vesicular 16_2SH^a

$10^3[16_2SH], M$	k_p for substrate, ^b s^{-1}			
	PNPA ^c	PNPB	ANBS	PNPP
0.23	0.44			
0.25		8.19	4.88	
0.30				20.0
0.38		9.81	6.54	
0.45	1.06			
0.50		11.3	6.99	
0.75		12.4	7.33	21.7
0.90	1.42			
1.0		13.2	6.70	
1.4	2.98			
1.5		13.4	6.32	21.3
1.8	4.0			
3.6	4.9			
5.0		7.59	6.38	
6.4	1.86			

^aFor conditions, see text. ^bEntries are mean values of 3–5 runs. Reproducibilities are better than $\pm 3\%$ in all cases. ^cData taken from ref 18.

$k_p = 2.4 s^{-1}$ at $[16_2SH] = 1.0 \times 10^{-3} M$ and pH 8.1.

In order to compare the esterolytic properties of vesicular 16_2SH with those of micellar $16SH$ (**3**),²¹ a rate constant vs. $[16SH]$ profile was similarly determined for the $16SH/PNPB$ reaction in 0.01 M Tris buffer (other conditions as above). The profile appears in Figure 2, where $k_p^{max} = 4.8 \pm 0.1 s^{-1}$ at $[16SH] = 2.5 \times 10^{-3} M$. Previously, we reported²¹ $k_p^{max} = 6.68 \pm 0.03 s^{-1}$ at $[16SH] = 6.4 \times 10^{-3} M$ in 0.02 M phosphate buffer at pH 7.0, $\mu = 0.05$ (KCl). The maximum rate constant for $16SH$ micellar cleavage of PNPB appears to be marginally smaller in Tris than in phosphate buffers.

Finally, rate constants (k_0) for the unaugmented, slow cleavages of PNPA, PNPB, and ANBS in pH 8 Tris buffer were determined to be 4.5×10^{-5} , 3.5×10^{-5} , and $4.0 \times 10^{-5} s^{-1}$, respectively.

Early Stage of Esterolysis. Above, we indicated that stopped-flow combination of a pH 2 16_2SH vesicular solution with an equal volume of a 0.02 M Tris buffer solution containing $5 \times 10^{-5} M$ PNPB (final pH 7.7) led to a triphasic absorption vs. time correlation for the release of $PNPO^-$. An example of this behavior appears in Figure 3. In this section, we will deal with the zero-order absorption increase that occurs within the initial 200 ms of reaction (points A to B in Figure 3); the fast exponential absorbance increase (points B to C) represents the conventional $16_2SH/PNPB$ cleavage reaction and was examined in the preceding section.

Zero-order behavior was observed only with the very hydrophobic PNPB and PNPP substrates that are strongly bound to the 16_2SH vesicles and are cleaved with high values of k_p^{max} ($>10 s^{-1}$; see Table II). At $[16_2SH] = 1.0\text{--}1.5 \times 10^{-3} M$, $[substrate]$

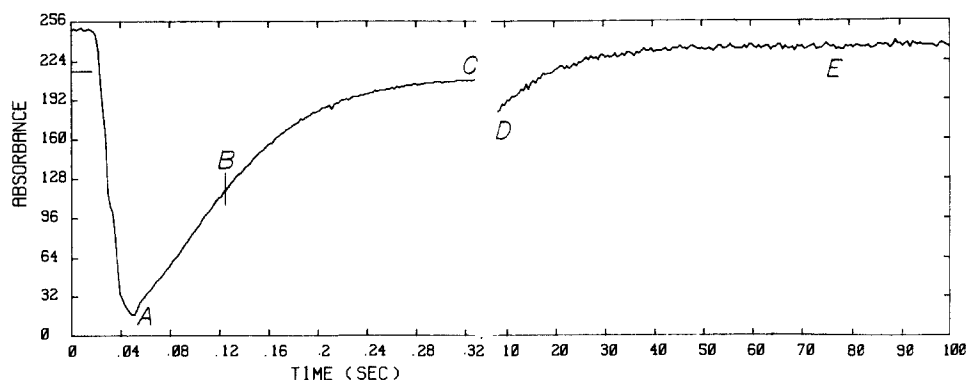


Figure 3. Three-syringe, stopped-flow reaction of (final conditions) $1.5 \times 10^{-3} M$ vesicular 16_2SH and $2.5 \times 10^{-5} M$ PNPB at pH 2 (HCl) [syringes A and B] with 0.01 M Tris/0.005 M KCl at pH 8 [syringe C]. The pH after mixing was 7.7. Absorbance (arbitrary units, ordinate) is plotted vs. time (s, abscissa); note the discontinuity on the time axis after 0.32 s. Data collection begins at point A (~ 0.05 s), after the observation cuvette has been filled. From points A to B, absorbance vs. time is zero order; from B to C the relationship is first order (fast exponential). The slower process (points D to E) is artifactual. See text for discussion. Although this reaction was run on a three-syringe device, syringes A and B were filled with identical solutions, so that, except for a ~ 50 -ms delay in filling the observation cuvette, the experiment is equivalent to a two-syringe, stopped-flow experiment.

Table III. Percent Zero-Order Reaction vs. Age Time^a

age time, ms	% zero-order reaction
<2 ^b	51
47	50
87	32
137	24
237	0

^aFinal conditions: 0.01 M Tris buffer, pH 7.7 ± 0.2, 4 vol% ethanol, 0.4 vol% CH₃CN, 0.75 × 10⁻³ M KCl, 25 ± 0.5 °C, [16₂SH] = 0.5 × 10⁻³ M, [PNPH] = 2.5 × 10⁻⁵ M. ^bTwo-syringe experiment. All other runs refer to the three-syringe modification; see text.

Table IV. Rate Constants vs. Aging for 16₂SH Cleavage of PNPH and PNPA^a

run	age time, s	k_{ψ} , s ^{-1b}	
		PNPH ^c	PNPA ^d
1	0.047	11 ± 1.4	1.02 ± 0.01 ₂
2	0.087	12 ± 1.9	1.00 ± 0.06 ₃
3	0.137	12.6 ± 1.2	0.99 ± 0.03 ₃
4	0.237	12.5 ± 0.5	
5	0.437	15.3 ± 1.1 ₄ ^e	
6	0.537		0.97 ± 0.01 ₂
7	0.637	14.9 ± 0.4 ^e	
8	1.04	14.0 ± 0.9	0.96 ± 0.01 ₂
9	2.04	13.7 ± 0.3 ^e	
10	5.04	12.7 ± 0.2 ^e	0.76 ± 0.01 ₂
11	7.04	12.3 ± 0.3 ^e	
12	10.0	11.0 ± 0.1	0.65 ± 0.01 ₂

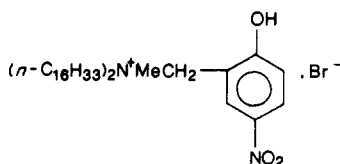
^aFor conditions, see Table III, footnote a. ^bErrors are average deviations of the mean values of k_{ψ} for 2 to 3 independent vesicle preparations. The average deviation of k_{ψ} within each preparation was within ±0.5. ^cErrors are average deviations of n (subscript) determinations on a single vesicle preparation. ^dSingle vesicle preparation.

= 2–4 × 10⁻⁵ M, pH 7.5 ± 0.2, and other conditions as described above, typical zero-order rate constants were 13.0 ± 0.3 × 10⁻⁵ and 8.6 ± 0.6₃ × 10⁻⁵ mol/(L·s), respectively, for PNPH and PNPP. These processes accounted for ~50% of the total ΔA.

To learn if these effects were related to the 2.0 to 7.7 pH jump that accompanied vesicle/substrate mixing, we examined the PNPH/16₂SH reaction on a three-syringe modification of the stopped-flow spectrophotometer. In this configuration, 2.0 × 10⁻³ M vesicular 16₂SH at pH 2 was rapidly (<1 ms) mixed with Tris buffer, bringing the pH to ~7.7. Next, the resulting solution was "aged", and then it was rapidly mixed (<1 ms) with a Tris buffer solution of PNPH. The final solution was followed spectrophotometrically for the release of PNPO⁻. As shown in Table III, the percent contribution of the zero-order reaction to the total absorbance change decreased with increasing aging time and disappeared entirely after ~200 ms of aging.

Table IV (runs 1–4) shows that the value of k_{ψ} for the normal pseudo-first-order PNPH reaction (see above) is effectively constant throughout this period. At somewhat longer aging times (400–600 ms, runs 5–7), k_{ψ} increases slightly. After still more aging, k_{ψ} declines (runs 9–12). The last phenomenon could be associated with SH to S–S oxidation of the 16₂SH vesicles; cf. the discussion of ANS fluorescence, above.

The zero-order kinetics are not observed when the 16₂SH is first "incubated" for 200 ms at pH 7.7, so that this phenomenon must be associated with changes in the 16₂SH vesicles as the pH jumps from 2 to 7.7 and the vesicular surfactant largely deprotonates to 16₂S⁻. We asked whether "slow" deprotonation of the vesicular SH groups to their reactive S⁻ form could be involved. To investigate this possibility, we prepared vesicles of 16₂SH or 16₂OH that contained 3 mol % of the indicator surfactant 16.³⁴



16

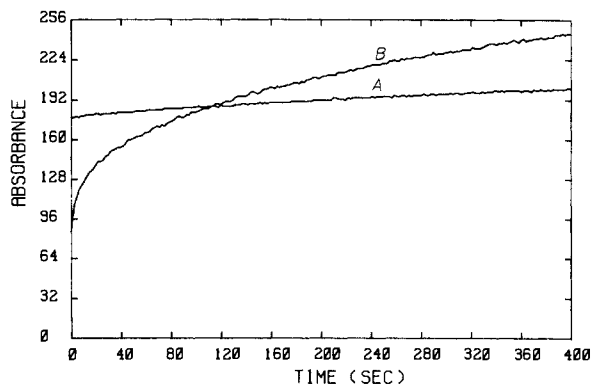


Figure 4. Stopped-flow combination of 2 × 10⁻³ M vesicular 16₂OH (A) or 16₂SH (B), each containing 3 mol % of 16, at pH 2.0, with 0.02 M Tris free base. The final pH was 7.7. The absorbance at 400 nm of the *p*-nitrophenoxide form of 16 (arbitrary units) is plotted vs. time (s). See text for other conditions and discussion.

The pK_a of 16 (50 mol % in 16₂OH) is 4.5 ± 0.2₃, as determined spectrophotometrically at 400 nm by titration with standardized base, and it is known that 16 (in nonfunctional) dihexadecyldimethylammonium vesicles is immediately ($k_{\psi} > 500$ s⁻¹) deprotonated to its *p*-nitrophenoxide form when the solution pH is raised from 3.0 to 8.5.³⁴

Figure 4 shows the results of two-syringe, stopped-flow combinations of pH 2.0, 2.0 × 10⁻³ M 16₂OH or 16₂SH vesicles, containing 3 mol % 16, with 0.02 M Tris free base. All solutions are 0.01 M in KCl, and the absorbance is followed at 400 nm. With 16₂OH/16, the *p*-nitrophenoxide form of 16 appears "instantaneously" as the pH jumps to 7.7. There follows a slow, artifactual absorbance increase (~10–15% over 7 min) that we attribute to light scattering originating in osmometric vesicular changes (see below). The behavior of the 16₂SH/16 system is qualitatively different; more time appears to be required here for complete deprotonation of 16 than in the case of 16₂OH vesicles. Absorbance increases due to vesicle alteration by S⁻ to S–S oxidation (see above), or by osmometric changes, should be significant only at times longer than ~10 s. Allowing for these effects, we are left in the 16₂SH/16 case with measurably slow absorbance changes (~25% of the total) that occur within 10 s of the pH jump. Therefore, because the zero-order kinetic process in the 16₂SH/PNPH reaction is restricted to the initial 200 ms, we cannot exclude slow deprotonation of the 16₂SH vesicles as a contributory factor. We will return to this problem in the Discussion section.

Late Stage of Esterolysis. When vesicular 16₂SH reacts with PNPA, a slow, apparently first-order absorbance increase follows the fast exponential change that corresponds to the liberation of PNPO⁻.¹⁸ The slow phase accounts for ~4–10% of the total ΔA and lasts for ~200 s ($k_{\psi} \sim 0.03$ – 0.08 s⁻¹), whereas the major reaction is finished within ~0.5 s ($k_{\psi} = 4.9$ s⁻¹ at [16₂SH] = 3.6 × 10⁻³ M, pH 7.5).³⁵ Similar phenomena attend the reactions of vesicular 16₂SH with PNPH (see above, Figure 3), ANBS, or PNPP.

Initially, we attributed the fast and slow exponential processes in the 16₂SH/PNPA reaction to exovesicular and endovesicular reactions, respectively.¹⁸ Analogous behavior was observed in the cleavage of reactive phosphate esters at high pH and was similarly rationalized.³⁶ More recently, the latter examples were recognized to be artifactual, with the slow absorbance changes most likely due to osmometric changes in the vesicles that accompany stopped-flow mixing.³³ We have, therefore, performed a series of control experiments designed to check the origin of the slow kinetic phase in the 16₂SH esterolyses.

(34) Moss, R. A.; Schreck, R. P. *Tetrahedron Lett.* **1985**, 26, 6305.

(35) These phenomena are illustrated in Figure 2 of ref 18.

(36) Moss, R. A.; Ihara, Y.; Bizzigotti, G. O. *J. Am. Chem. Soc.* **1982**, 104, 7476.

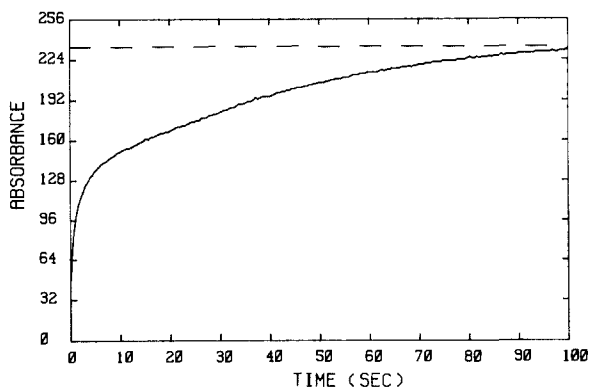


Figure 5. Absorbance (arbitrarily expanded scale) at 400 nm vs. time (s) for the stopped-flow combination of 2×10^{-3} M vesicular 16_2SH at pH 2 with 1×10^{-4} M *p*-nitrophenoxide ion in 0.02 M Tris buffer, final pH 7.7. See text for other conditions and discussion.

Vesicular solutions of 2.0×10^{-3} M 16_2SH at pH 2 (HCl) and 0.01 M KCl were mixed in the stopped-flow spectrometer with equal volumes of aqueous 0.02 M Tris buffer containing 0.01 M KCl, 1×10^{-4} M *p*-nitrophenoxide ion, and 1×10^{-4} M acetate or hexanoate ions. These controls bring together the 16_2SH vesicles, and the chromophoric product ion of their reactions with PNPA or PNPB, under conditions similar to those of the actual reactions. Absorbance was monitored at 400 nm as a function of time.

Figure 5 shows the absorbance/time display for the $\text{PNPO}^-/\text{AcO}^-$ control, and it is also representative of the $\text{PNPO}^-/\text{hexanoate}$ runs. In all cases, we observe an instantaneous absorbance upon admission of PNPO^- to the observation cuvette. Subsequently, over 1–2 min, there is a gradual 5–15% absorbance increase, and then the signal stabilizes. "Rate constants" derived by standard computational methods from the time-dependent data appear to be first order, with " k_ψ " ~ 0.02 – 0.06 s^{-1} and correlation coefficients of 0.997–0.999 for data sets of 100–150 points. The data of Figure 5 (at a time > 5 s), for example, lead to $k_\psi = 0.026 \pm 0.001_4$ s^{-1} and $r_{av} = 0.999$.

Slow exponential behavior can thus be observed in the absence of substrate, so that the phenomenon is not necessarily indicative of slow esterolysis reactions. More likely, it is an artifact caused by time-dependent osmometric effects that induce vesicular growth or fusion accompanied by enhanced light scattering. These processes mimic the time-dependent 400-nm absorbance characteristic of the slower esterolytic reactions.³⁷

Discussion

The realization that the slow kinetic processes observed in the reactions of vesicular 16_2SH with various active esters are probably artifacts leaves no evidence for kinetically resolvable endovesicular reactions. It is most reasonable to conclude that the present substrates, 11–15, are able to rapidly transit the outer 16_2S^- bilayer at pH 8 and to react equally well at exovesicular and (probably some) endovesicular sites. The half time for the fastest ANBS/ 16_2SH reaction from Table II ($k_\psi = 7.3$ s^{-1}) is ~ 95 ms, considerably longer than the permeation half time in 16_2S^- of the similarly hydrophobic, anionic, fluorescent sulfonate probe ANS, $\tau_{1/2} \sim 11$ ms at pH 7.7 (Table I). Even the fastest reaction of Table II, that between 16_2S^- and PNPP, has $k_\psi \sim 22$ s^{-1} and $\tau_{1/2} \sim 31$ ms, ~ 3 times longer than $\tau_{1/2}$ for ANS permeation. Therefore, the fluorescence results support the suggestion that ANBS (and the other substrates) crosses the outer vesicular membranes more rapidly than it reacts with the thiolate groups that are covalently bound to those membranes.

Although we do not find evidence for permeation-limited reactions, there are unusual kinetic effects at very short reaction

times that are observable when the more hydrophobic substrates at pH 8 are rapidly mixed with 16_2SH vesicles at pH 2. The ensuing zero-order cleavage reactions, and PNPO^- release, account for up to $\sim 50\%$ of the total reaction. When, however, the 16_2SH vesicles are first incubated at pH 7.7 for 200 ms before the addition of the substrate, the zero-order kinetics vanish; only the rapid pseudo-first-order cleavage reaction is observed (cf. Table III). We should also note that the reactions of 16_2Im (1) with PNPB display no zero-order behavior even though they are as rapid as the analogous 16_2SH reactions.¹⁶ The 16_2Im reactions, however, are carried out completely at pH 8, without the imposition of a pH jump during stopped-flow mixing.

In the short, zero-order kinetic regime following the simultaneous combination of 16_2SH , PNPB, and Tris buffer, the rate-limiting event is, therefore, not the attack of 16_2S^- on PNPB but rather a change in the vesicle from an inactive to a reactive form. The simplest rationale is that deprotonation of the inactive 16_2SH vesicles at pH 2 to the reactive 16_2S^- species at pH 7–8 is slow, i.e., requires milliseconds. Hydrophobic substrates will bind to the vesicles much more rapidly,^{31,38} so that at very short reaction times, when there is a large excess of bound substrate and few S^- groups, the $\text{SH} \rightarrow \text{S}^-$ conversion will be limiting. Moreover, because stopped-flow mixing changes the bulk pH of the vesicular solution from 2 to 7.7 within 1 ms, the deprotonation should proceed at a "constant" rate. After deprotonation, when $[\text{S}^-] > [\text{substrate}]$, pseudo-first-order kinetics are observed, and the attack of S^- on the substrate is limiting.

Some support for this simple scenario can be derived from the indicator experiments with 16 (see above and Figure 4). These are consistent with a slow deprotonation phenomenon on a seconds time scale. Nevertheless, the majority of the deprotonation ($\sim 75\%$) in these experiments seems to occur within the ~ 1 -ms mixing time of the stopped-flow unit. Therefore, simple deprotonation is probably not the sole component of the rate-determining event at short reaction times.

Deprotonation not only converts SH to S^- , but it also alters vesicular charge from cationic to largely zwitterionic, with major consequences for vesicular structure (e.g., the apparent increase in diameter from ~ 300 to 1000 Å, see above). Accompanying the deprotonation and structural change, we may imagine conformational reorientation of the neutral $\text{CH}_2\text{CH}_2\text{SH}$ functional groups after their conversion to the mutually repulsive $\text{CH}_2\text{CH}_2\text{S}^-$ moieties. Therefore, even if SH deprotonation were much faster than the thiolysis reaction, relaxation of the vesicles in response to the new equilibrium conditions, and the concomitant conformational redeployment of their functional groups, could occur on the millisecond time scale and be rate limiting. Presently, both explanations of the zero-order kinetics remain conjectural, although it is clear that optimal conditions for the conventional reaction of PNPB with 16_2SH vesicles are not attained concurrently with the pH jump but require several hundred milliseconds to evolve (cf. Tables III and IV).

The fast exponential 16_2SH thiolyses of PNPA, PNPB, and ANBS obey typical rate constant/[surfactant] profiles^{1a,2} (cf. Table II and Figure 1). Similar behavior attends the micellar reactions of 16_2SH with these substrates (cf. ref 21 and Figure 2). We applied Lineweaver–Burk analysis³⁹ to the data in Table II and Figures 1 and 2, obtaining values for k , or k_m , the cleavage rate constants for substrates fully bound to the vesicular or micellar aggregates, as well as K/N , the ratio of the binding constant to the vesicular or micellar aggregation number. For this analysis, we used the substrate/buffer k_0 values reported above (see the Results section), and took a critical micelle concentration (cmc) of ~ 0 M for vesicular 16_2SH and a "best-fit" cmc of 1.0×10^{-5} M for the $16\text{SH}/\text{PNPB}$ micellar reaction.⁴⁰ The derived kinetic parameters, together with the maximum observed rate constants

(38) See ref 2, Chapter 6, especially pp 155–158.

(39) See ref 1a, Chapter 4.

(40) In contrast to the $16\text{SH}/\text{PNPB}$ reaction in phosphate buffer, where the cmc was observed kinetically at $[16\text{SH}] = 3.3 \times 10^{-4}$ M,²¹ an exact value could not be determined in Tris buffer (see Figure 2). The kinetic cmc appears to be an order of magnitude lower in Tris than in phosphate buffer.

(37) Such phenomena are well described: Casmona Ribeiro, A. M.; Chalmovich, H. *Biochim. Biophys. Acta* 1983, 733, 172. Carmona Ribeiro, A. M.; Yoshida, L. S.; Sessa, A.; Chalmovich, H. *J. Colloid Interface Sci.* 1984, 100, 433.

Table V. Kinetic Parameters for Reactions of Surfactants 16₂SH and 16SH^a

reaction	k_v^{\max} , s ^{-1b}	k_{cat} , L/(mol·s) ^c	k_{agg} , s ^{-1d}	K/N , M ^d
16 ₂ SH/PNPA ^e	4.9 [3.6]	1360	9.8	276
16 ₂ SH/PNPH ^e	13.4 [1.5]	8930	16.3	4130
16 ₂ SH/ANBS ^e	7.33 [0.75]	9770	10.7	3560
16SH/PNPH ^f	4.75 [2.5]	1900	5.66	2190
16 ₂ Im/PNPH ^{e,g}	16.3 [3.4] ^h	4790	16.8	2400

^a Conditions: 0.01 M Tris buffer, pH 7.7, 0.01 M KCl, 25 °C.

^b Value in brackets is 10³[surfactant], M, at which k_v^{\max} was observed.

^c $k_{cat} = k_v^{\max}/[\text{surfactant}]$. ^d From the Lineweaver-Burk analysis of the data in Table II and Figure 2. ^e Vesicular reaction. ^f Micellar reaction. ^g From ref 16. ^h At the maximum solubility of 16₂Im but not at true k_v^{\max} ; see ref 16, Figure 1.

(from Table II or Figure 2), are presented in Table V.

The data of Table V support the contention that vesicular 16₂SH is an extraordinarily potent esterolytic reagent. Its reactivity toward PNPH is very similar to that of 16₂Im, which is itself more reactive than previously reported micellar imidazole-functionalized surfactants.¹⁶ Toward active ester substrates, vesicular 16₂SH is 2–3 times more reactive than its micellar analogue, 16SH, one of the most reactive esterolytic micellar reagents.²¹ (An extensive survey of the comparative reactivities of functional micellar reagents has been published.²¹) Defining k_{cat} as $k_v^{\max}/[\text{surfactant}]$, $k_{cat} = 1360$ L/(mol·s) for vesicular 16₂SH and PNPA, which is comparable to the reactivity of heptanethiol/R₂N⁺Me₂ (R = 85% *n*-C₁₈, 15% *n*-C₁₆) vesicles with the same substrate.^{17a,41}

The vesicular > micellar kinetic advantage, observed with both SH¹⁷ and Im¹⁶ reagents, presumably reflects the greater binding capacity of vesicles over micelles; aggregation numbers (N) for vesicles are larger than for micelles,² as are K/N values (Table V and ref 16) and therefore K .

From Table V, the order of substrate reactivity toward 16₂SH is PNPH > ANBS > PNPA. The greater reactivity of PNPH (vs. PNPA) is due to its greater hydrophobicity and consequent stronger binding to the vesicles. This is supported by the much larger value of K/N for PNPH; similar behavior was observed in 16₂Im esterolysis reactions.¹⁶ However, with the imidazole functional vesicles, ANBS was slightly more reactive than PNPH ($k_{agg} = 17.4$ vs. 16.8 s⁻¹), even though it was not as strongly bound ($K/N = 1150$ vs. 2400 M).¹⁶ Here, with 16₂SH, PNPH appears both more reactive and more strongly bound than ANBS. The origins of these effects are unclear, although we note that the electrostatic interactions between anionic ANBS and cationic 16₂Im could be more specific than those between ANBS and the zwitterionic 16₂S⁻.

We agree with Cuccovia et al.^{17b} that the principal origin of the extraordinarily rapid thiolyses observed with reagents like vesicular 16₂SH must lie in the restriction of the nucleophilic reagent and the substrate to very small volume elements within the vesicles. This concentration effect⁴² or "dimensional restriction"^{17b} may be worth upwards of 10⁴ s⁻¹ in k_v , even with nonspecific binding of the substrate.

With the development of functional vesicle-forming surfactants such as 16₂SH and 16₂Im, we appear to have optimized the balance between the esterolytic kinetic potency and molecular simplicity of the reagent. Our attention now shifts to the synthesis of appropriately functionalized lipids, where the glycerol ester based hydrophobic backbone of the derived liposomes may permit greater control over substrate or reagent permeation, enabling us to make better and more specific use of the high reaction rates available in these molecular assemblies.

(41) On the basis of [heptanethiol], we estimate $k_{cat} \sim 1460$ L/(mol·s) from the data in ref 17a; cf. the caption of Figure 2 in that reference.

(42) This point has been well established in micellar chemistry by C. A. Bunton. See, for example: Bunton, C. A. *Catal. Rev.—Sci. Eng.* **1979**, *20*, 1. See also: Cipiciani, A.; Germani, R.; Savelli, G.; Bunton, C. A. *Tetrahedron Lett.* **1984**, *25*, 3765.

Experimental Section⁴³

Materials. PNPA (**11**) was obtained from Sigma and recrystallized from absolute EtOH; mp 78.5–79 °C [lit.^{44a} mp 79–80 °C]. PNPH (**12**), PNPP (**13**), and DPPC (**9**) were purchased from Sigma and used as received. ANBS (**14**) was prepared from *o*-nitrophenol via sodium 4-hydroxy-2-nitrobenzenesulfonate⁴⁵ by the procedures of Overberger and Letsinger⁴⁶ and was recrystallized from 85:15 acetic acid–benzene before use, mp >300 °C.⁴⁶ ANB (**15**) was prepared by the method of Overberger et al.⁴⁷ and recrystallized 3 times from benzene, mp 145.5–146 °C [lit.⁴⁷ mp 152 °C]. Our sample was homogeneous to TLC. Indicator **16** was available from another study.³² ANS (**10**), dithiothreitol, Tris buffer, and hexanoic acid (Gold Label) were all obtained from Aldrich Chemical Co. and used as received. *p*-Nitrophenol was obtained from Matheson Co. and was recrystallized from toluene, mp 114.5–116.5 °C [lit.^{44b} mp 114 °C].

***N,N*-Dihexadecyl-*N*-methyl-*N*-(2-mercaptoethyl)ammonium Chloride (16₂SH, **2**).** Hydroxy surfactant 16₂OH (**4**)²³ (10.7 g, 17.7 mmol) was dissolved in 75 mL of dry CH₂Cl₂ and 1.43 mL (1.40 g, 17.7 mmol) of pyridine. A solution of 12.5 g (44.3 mmol) of trifluoromethanesulfonic anhydride in 75 mL of dry CH₂Cl₂ was added, and the solution was stirred for 60 min at room temperature. NMR spectroscopy then indicated conversion to the analogous triflate surfactant **5**.⁴⁸

Freshly distilled thioacetic acid (bp 86–89 °C; 16.14 g, 0.212 mol, Aldrich) was dissolved in 35 mL of water, and the pH was adjusted to 7.5 with 0.2 M NaOH. This solution was added to the triflate surfactant solution, and the two-phase mixture was vigorously stirred for 16 h at room temperature. The CH₂Cl₂ layer and two 30-mL CH₂Cl₂ washes of the aqueous layer were combined and dried over MgSO₄. After removal of the MgSO₄, the bulk of the CH₂Cl₂ was removed under vacuum to give a light-brown oil. Adding 200 mL of dry diethyl ether followed by standing at –5 °C for 16 h produced a precipitate. Filtering the precipitate, washing it with cold, dry diethyl ether, and drying it under vacuum gave 10.68 g (14.6 mmol, 82.5% yield) of *N,N*-dihexadecyl-*N*-methyl-*N*-(2-(acetylthio)ethyl)ammonium trifluoromethanesulfonate (**6**): mp 73–76 °C; NMR (CDCl₃, Me₄Si) δ 0.87 (t, 6 H, 2Me), 1.27 (s, 56 H, [(CH₂)₁₄]), 2.37 (s, 3 H, CH₃COS), 3.18–3.30 (m, 11 H, (CH₂)₂N⁺(CH₃)CH₂CH₂S); IR (thin film) 2925, 2850, 1700, 1465, 1260, 1160, 1035 cm⁻¹.

Dowex 1-X8 ion-exchange beads in the chloride form (38.8 g, 0.163 equiv, J. T. Baker) and 10.68 g (14.6 mmol) of triflate surfactant **6** were mixed in 200 mL of 80% aqueous ethanol and heated to 75 °C for several minutes. The beads were filtered off and washed with three 50-mL portions of hot 2-propanol. The 2-propanol was removed under vacuum and the residue taken up in approximately 10 mL of 80% ethanol. This solution was added to the original ethanol filtrate. The entire ion-exchange process was then repeated 2 more times with 38.2-g (0.160-equiv) and 38.6-g (0.162-equiv) portions of the Dowex beads. When the complete process was finished, the combined filtrates were concentrated under vacuum to give a yellowish residue of chloride **7**. This was recrystallized twice from 20:1 isooctane–diethyl ether⁴⁹ and dried under high vacuum to afford 7.20 g (11.64 mmol, 80% yield) of 16₂SACl⁻ (**7**); mp 144–147 °C, liquid crystal 48–50 °C; NMR (CDCl₃, Me₄Si) δ 0.88 (t, 6 H, 2Me), 1.26 (s, 56 H, [(CH₂)₁₄]), 2.37 (s, 3 H, CH₃COS), 3.43 (m, 11 H, (CH₂)₂N⁺(CH₃)CH₂CH₂S); IR (thin film) 3300 (0.75H₂O), 2925, 2850, 1685, 1465, 1135 cm⁻¹; the 1260-, 1160-, and 1035-cm⁻¹ trifluoromethanesulfonate bands were absent in the IR spectrum of this compound.

Anal. Calcd for C₃₇H₇₆ClNO₂·0.75H₂O: C, 70.31; H, 12.36; Cl, 5.61. Found: C, 70.30; H, 12.46; Cl, 6.22.

The thioacetate surfactant **7** (0.229 g, 0.36 mmol) was dissolved in 20 mL of absolute ethanol which had been refluxed under vacuum for 60 min to remove oxygen. Concentrated HCl (7 mL) was added to give a solution of 3 N HCl in 75% aqueous ethanol. The solution was refluxed under nitrogen for 3 h. The HCl was removed from the hot solution

(43) Melting points are uncorrected. IR spectra were recorded on a Perkin-Elmer Model 727B instrument. NMR spectra were determined on a Varian T-60 instrument. Microanalyses were done by Robertson Laboratory, Florham Park, NJ.

(44) (a) *Handbook of Chemistry and Physics*, 45th ed.; Weast, R. C., Ed.; Chemical Rubber Publishing: Cleveland, OH, 1964; p C-85, (b) p C-470.

(45) Gnehm, R.; Knecht, O. *J. Prakt. Chem.* **1906**, *73*, 519.

(46) Overberger, C. G.; Okamoto, Y. *Macromolecules* **1972**, *5*, 363. Letsinger, R. L.; Saveriede, T. J. *J. Am. Chem. Soc.* **1962**, *84*, 3122.

(47) Overberger, C. G.; St. Pierre, T.; Vorchheimer, N.; Lee, J.; Yaroslavsky, S. *J. Am. Chem. Soc.* **1965**, *87*, 295.

(48) The CH₂O absorbance of **4** at δ 4.10 was replaced by the CH₂OTf peak at δ 5.03, and the hydroxyl proton peak disappeared.

(49) This compound requires water for crystallization. Therefore, the first recrystallization mixture must stand open to the atmosphere for ca. 24 h in order to absorb the water; otherwise crystals will not form.

under aspirator vacuum, and the ethanol was removed under 8-mmHg vacuum. The resulting aqueous slurry was lyophilized to a dry white powder. The product was recrystallized from ethyl acetate to afford 0.170 g (0.295 mmol, 81% yield) of $16_2\text{SH}\cdot\text{Cl}^-$ (2): mp 129–132 °C; the free SH activity was $101 \pm 2\%$ by Ellman's assay;^{25,50} NMR (CDCl_3 , Me_4Si) δ 0.88 (t, 6 H, 2Me), 1.27 (s, 56 H, $[(\text{CH}_2)_{14}]_2$), 3.4 (m, 12 H, $(\text{CH}_2)_2\text{N}^+(\text{CH}_3)\text{CH}_2\text{CH}_2\text{SH}$); the 3 H SCOCH_3 singlet of $16_2\text{SAC}\cdot\text{Cl}^-$ (δ 2.37) was absent in the spectrum of 16_2SH .

Kinetic Studies. The preparation of 16_2SH vesicles is described above (see the Results section). Two-syringe, stopped-flow reactions were followed with a Durrum (Dionex) Model D-130 spectrophotometer fitted with a Beckman DU-2 monochromator. Absorbance data were acquired by a photomultiplier tube linked to a custom-built 2048 channel, adjustable sampling time, A/D converter and thence to a Commodore Model 8032 microcomputer for disk storage. Kinetic analysis with custom-written software and high-resolution graphics employed either the 8032 or (later) a Commodore Model SP9000 "Super Pet" microcomputer. All pH measurements were made with a Radiometer Model 25 pH meter. Details of reagent concentrations, observed rate constants, reproducibilities, and reaction conditions appear in the Results section and in Table II.

Three-syringe, stopped-flow experiments made use of a Dionex Model D-132 multimixing unit, retrofitted to the Model D-110 stopped-flow

(50) 16_2SH that had been oxidized by exposure to air could be restored to quantitative Ellman's activity by recrystallization from ethyl acetate to which a slight excess of dithiothreitol had been added.

spectrophotometer. The data collection and analysis system was unchanged. Results of these experiments appear in Tables III and IV.

Fluorescence Experiments. Static fluorescence measurements were made with a SLM Model 4800 instrument equipped with a Xenon excitation lamp: excitation slit, 8 nm; emission slit, 0.5 nm. Data were collected with an Apple IIe computer and could be corrected for instrumental response. Output was digital or analog, as desired.

Stopped-flow fluorescence experiments employed the Durrum Model 110 instrument equipped with a special cuvette designed for emission at 90° to the probe beam. A Corning 3-72, 420-nm cutoff filter was inserted between the sample and the photomultiplier tube to screen out scattered excitation light. UV excitation was provided by an Osram 150-W xenon lamp powered by a Model DCR-150X (Gates and Co.) power supply. The excitation light was passed through a Beckman DU-2 monochromator set at 368 nm. Results of the fluorescence studies appear above and in Table I.

Acknowledgments.^{27,30} We are grateful to the U.S. Army Research Office and to the donors of the Petroleum Research Fund, administered by the American Chemical Society, for financial support.

Registry No. 2, 79246-00-7; 4 (R = $n\text{-C}_{16}\text{H}_{33}$), 83710-46-7; 5 (R = $n\text{-C}_{16}\text{H}_{33}$), 103322-05-0; 6 (R = $n\text{-C}_{16}\text{H}_{33}$), 103322-07-2; 7 (R = $n\text{-C}_{16}\text{H}_{33}$), 103322-08-3; Tf_2O , 358-23-6; $\text{CH}_3\text{COS}^-\text{Na}^+$, 34832-35-4; *p*-nitrophenyl acetate, 830-03-5; *p*-nitrophenyl hexanoate, 956-75-2; 4-acetoxy-3-nitrobenzenesulfonate, 103322-09-4; *p*-nitrophenyl palmate, 1492-30-4.

Gas-Phase Photochemistry of a β,γ -Unsaturated Ketone. Concerted and Radical Mechanisms of the 1,3-Acetyl Shift in 1,2-Dimethylcyclopent-2-enyl Methyl Ketone

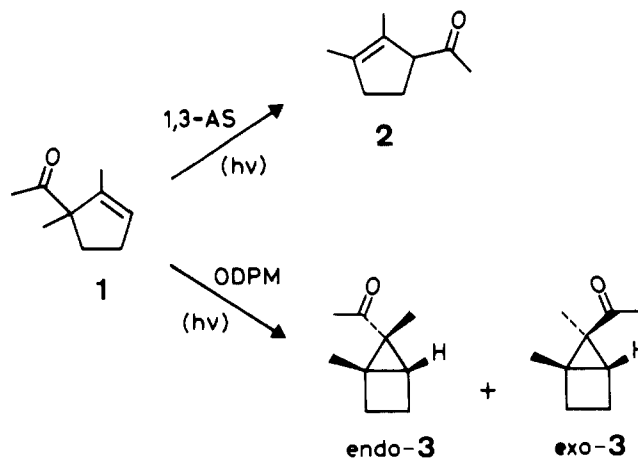
Bruno Reimann, David E. Sadler, and Kurt Schaffner*

Contribution from the Max-Planck-Institut für Strahlenchemie, D-4330 Mülheim a. d. Ruhr, West Germany. Received November 22, 1985

Abstract: The 1,3-acetyl shift of the photoexcited β,γ -unsaturated ketone 1,2-dimethylcyclopent-2-enyl methyl ketone has been investigated in the gas phase at room temperature and with 1 bar of CO_2 as a buffer gas. Roughly 25% of the total 1,3-acetyl shift reaction is shown to proceed in an orbital-symmetry-allowed concerted fashion from the first excited singlet state. The dominant primary reaction occurs by α -cleavage and recombination of the radicals, as it also does in liquid solution. The effects of radical scavenging and triplet quenching by added NO , O_2 , and *trans*-1,3-pentadiene served to differentiate between the concerted and radical recombination pathways and between the singlet and triplet excited-state origins of the products. The quenching of the triplet-generated oxa-di- π -methane rearrangement shows that the reaction is initiated in the lowest lying T_1 (π,π^*) state.

The solution photochemistry of β,γ -unsaturated ketones (β,γ -UKs) has been thoroughly investigated and extensively reviewed in recent years.¹ It is characterized by two reactions: the allylic 1,3-acetyl shift (1,3-AS) and the oxa-di- π -methane (ODPM) rearrangement. Photo-CIDNP, stereochemical experiments, and a combination of fluorescence lifetime and reaction quantum yield studies^{2a-c} have shown that the S_1 photochemistry of a model series of β,γ -UKs, the cyclopent-2-enyl methyl ketones, is dominated by one temperature-activated process leading, in part, to the 1,3-AS. Intersystem crossing populates both T_2 (n,π^*), which again undergoes the 1,3-AS,^{2d} and T_1 (π,π^*), which affords the

Scheme I. 1,3-AS (\rightarrow 2) and ODPM Rearrangement (\rightarrow 3) of 1,2-Dimethylcyclopent-2-enyl Methyl Ketone (1)



ODPM product.^{2d-f} On direct excitation the triplet reactions are only minor processes. For β,γ -UKs other than the above models

(1) Schuster, D. I. In *Rearrangements in Ground and Excited State*; de Mayo, P., Ed.; Academic Press: New York, 1980; Vol. 3, p 167.

(2) (a) Henne, A.; Slew, N. P. Y.; Schaffner, K. *J. Am. Chem. Soc.* **1979**, *101*, 3671; *Helv. Chim. Acta* **1979**, *62*, 1952. (b) Sadler, D. E.; Hildenbrand, K.; Schaffner, K. *Ibid.* **1982**, *65*, 2071. (c) Sadler, D. E.; Wendler, J.; Olbrich, G.; Schaffner, K. *J. Am. Chem. Soc.* **1984**, *106*, 2064. (d) Mirbach, M. J.; Henne, A.; Schaffner, K. *Ibid.* **1978**, *100*, 7127. (e) Tegmo-Larsson, I.-M.; Gonzenbach, H.-U.; Schaffner, K. *Helv. Chim. Acta* **1976**, *59*, 1376. (f) Gonzenbach, H.-U.; Tegmo-Larsson, I.-M.; Grosclaude, J.-P.; Schaffner, K. *Ibid.* **1977**, *60*, 1091. (g) Winter, B.; Schaffner, K. *J. Am. Chem. Soc.* **1976**, *98*, 2022. (h) Schaffner, K. *Tetrahedron* **1976**, *32*, 641; *J. Synth. Org. Chem. Jpn.* **1979**, *37*, 893.